NATIONAL ENERGY TECHNOLOGY LABORATORY

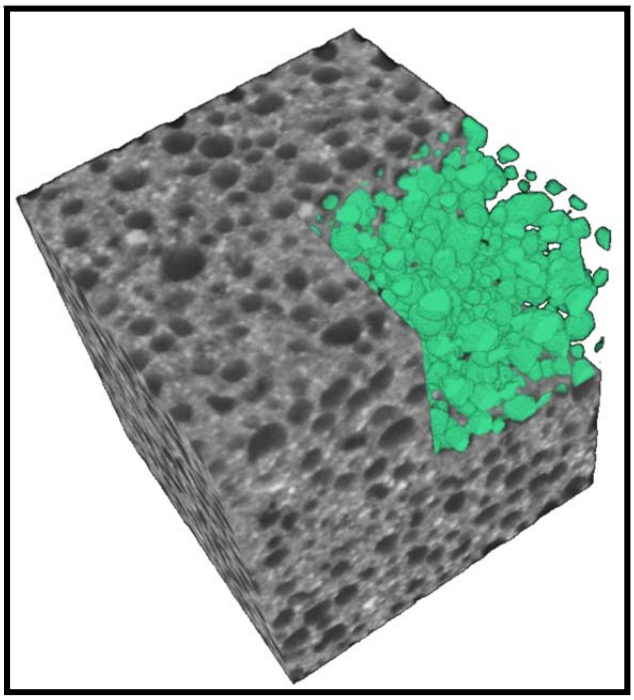

Addendum 1 to Computed Tomography and Statistical Analysis of Bubble Size Distributions in Atmospheric-Generated Foamed Cement

6 March 2014

U.S. DEPARTMENT OF ENERGY

Office of Fossil Energy

NETL-TRS-2-2014

Disclaimer

This report was prepared as an account of work sponsored by an agency of the United States Government. Neither the United States Government nor any agency thereof, nor any of their employees, makes any warranty, express or implied, or assumes any legal liability or responsibility for the accuracy, completeness, or usefulness of any information, apparatus, product, or process disclosed, or represents that its use would not infringe privately owned rights. Reference therein to any specific commercial product, process, or service by trade name, trademark, manufacturer, or otherwise does not necessarily constitute or imply its endorsement, recommendation, or favoring by the United States Government or any agency thereof. The views and opinions of authors expressed therein do not necessarily state or reflect those of the United States Government or any agency thereof.

Cover Illustration: 3-D rendering of a 3.12-mm^3 digital subsection of a 30% foam-quality cement sample, additive Recipe 2. One-eighth of the volume has been post-processed to isolate the gaseous voids within the foamed cement. The scan resolution is in 3.9 μm^3 per voxel.

Suggested Citation: Kutchko, B.; Moore, J.; Crandall, D.; Gill, M.; McIntyre, D.; Spaulding, R.; Strazisar, B.; Rosenbaum, E.; Haljasmaa, I.; Benge, G.; Cunningham, E.; DeBruijn, G.; Shine, J.; Gardner, C. *Addendum 1 to Computed Tomography and Statistical Analysis of Bubble Size Distributions in Atmospheric-Generated Foamed Cement*; NETL-TRS-2-2014; EPAct Technical Report Series; U.S. Department of Energy, National Energy Technology Laboratory: Morgantown, WV, 2014; p 20.

An electronic version of this report can be found at:
http://www.netl.doe.gov/research/on-site-research/publications and
https://edx.netl.doe.gov/udw

Addendum 1 to Computed Tomography and Statistical Analysis of Bubble Size Distributions in Atmospheric-Generated Foamed Cement

Barbara Kutchko[1], Johnathan Moore[2] (ORISE), Dustin Crandall[3], Magdalena Gill[3], Dustin McIntyre[2], Richard Spaulding[1] (NETL-RUA), Brian Strazisar[1], Eilis Rosenbaum[1], Igor Haljasmaa[4], Glen Benge[5], Erick Cunningham[6], Gunnar DeBruijn[7], Joe Shine[8], Craig Gardner[9]

[1] U.S. Department of Energy, Office of Research and Development, National Energy Technology Laboratory, 626 Cochrans Mill Road, Pittsburgh, PA 15236

[2] U.S. Department of Energy, Office of Research and Development, National Energy Technology Laboratory, 3610 Collins Ferry Road, Morgantown, WV 26507

[3] U.S. Department of Energy, National Energy Technology Laboratory, URS, 3610 Collins Ferry Road, Morgantown, WV 26507

[4] U.S. Department of Energy, National Energy Technology Laboratory, URS, 626 Cochrans Mill Road, Pittsburgh, PA 15236

[5] Benge Consulting, 86 E Slatestone Circle, The Woodlands, TX 77382

[6] BP America, 501 Westlake Boulevard, Houston, TX 77079

[7] Schlumberger, 300 Schlumberger Drive, Sugar Land, TX 77478

[8] Baker Hughes, 17021 Aldine Westfield Rd, Houston, TX 77073

[9] Chevron, 3901 Briarpark Drive, Houston, TX 77042

NETL-TRS-2-2014

6 March 2014

NETL Contacts:

Barbara Kutchko, Principal Investigator

Kelly Rose, Technical Coordinator

George Guthrie, Focus Area Lead

This page intentionally left blank.

Table of Contents

ABSTRACT **1**
1. INTRODUCTION **2**
2. METHODS **3**
2.1 CEMENT SLURRY PREPARATION 3
2.2 CEMENT CORE PREPARATION 3
2.3 CT SCANNING 5
2.4 DIGITAL IMAGING AND STATISTICAL ANALYSIS 5
3. RESULTS **7**
4. DISCUSSION **11**
5. REFERENCES **12**

List of Figures

Figure 1: Photographs of 25.4- and 6-mm diameter cores of 10% foam-quality FCR2 foamed cement Recipe 2 cores. 3
Figure 2: Photographs of 25.4- and 6-mm diameter cores of 20% foam-quality FCR2 foamed cement Recipe 2 cores. 4
Figure 3: Photographs of 25.4- and 6-mm diameter cores of 30% foam-quality FCR2 foamed cement Recipe 2 cores. 4
Figure 4: Photographs of 25.4- and 6-mm diameter cores of 40% foam-quality FCR2 foamed cement Recipe 2 cores. 4
Figure 5: 2-D slices of reconstructed 13.9-µm resolution CT scans of the 25.4-mm diameter samples of 10%, 20%, 30%, and 40% foam-quality FCR2 foamed cement Recipe 2 cores (left to right). 5
Figure 6: 2-D slices of reconstructed 3.9-µm resolution CT scans of the 6-mm diameter samples of 10%, 20%, 30%, and 40% foam- quality FCR2 foamed cement Recipe 2 cores (left to right). 5
Figure 7: CT-derived porosity vs. entrained air fraction with the dashed line denoting a linear relationship with slope = 1. The data are from low-resolution (macro) and high-resolution (micro) scans of both foamed cement recipes. 7
Figure 8: Log-log BSD plots of the 30% foam-quality samples. For the FCR1 and FCR2 foamed cement recipes, the micro- and macro-BSD are extremely similar. 8
Figure 9: Log-log BSD plots of the 10%, 20%, and 40% foam-quality samples. For the FCR1 and FCR2 foamed cement recipes, the micro- and macro-BSD have similar distributions. In all cases, the microscans captured a larger number of small bubbles, and the remaining BSD occupied a smaller percentage of the total bubbles. 9
Figure 10: Log-log BSD plots for the FCR1 and FCR2 foamed cement recipes with the BSDs overlaid. Scan resolutions for the FCR1 and FCR2 foamed cement recipe cores are 13.5 µm for the macroscans. The FCR1 microscans have a resolution of 3.7 µm and the FCR2 microscan resolutions are 3.9 µm. A) 10% foam quality, B) 20% foam quality, C) 30% foam quality, and D) 40% foam quality. 10

List of Tables

Table 1: Scan resolutions and resultant analysis volumes for FCR1 and FCR2 foamed cement recipe cores 6

Acronyms, Abbreviations, and Symbols

Term	Description
µm	Micrometer, 10^{-6} meter
2-D	Two-dimensional
3-D	Three-dimensional
API	American Petroleum Institute
BSD	Bubble size distribution
CT	Computed tomography
FCR1	Foamed cement Recipe 1
FCR2	Foamed cement Recipe 2
REV	Representative elemental volume
ROI	Region of interest

Acknowledgments

This work was completed as part of National Energy Technology Laboratory (NETL) research for the Department of Energy's Complementary Research Program under Section 999 of the Energy Policy Act of 2005. The authors wish to acknowledge Roy Long (NETL Strategic Center for Natural Gas and Oil) and Elena Melchert (DOE Office of Fossil Energy) for programmatic guidance, direction, and support.

The authors would like to thank Bryan Tennant, Karl Jarvis and Roger Lapeer for making the CT scanner lab functional. A special thanks to Jim Fazio for superior laboratory assistance.

This page intentionally left blank.

ABSTRACT

In this research study, NETL, working with the American Petroleum Institute (API) Subcommittee 10, Work Group 3, is using laboratory- and field-generated foamed cement samples for direct observation to characterize gas distribution. An important step in this research is developing accurate high-resolution imaging techniques. As was discussed in Kutchko et al. (2013), NETL researchers successfully produced high-resolution X-ray computed tomography (CT) three-dimensional (3-D) images of atmospheric-generated foamed cement across a range of foam qualities. When these foamed cements are used in the field, various foaming agents and stabilizers are used to promote the stability of bubbles within the cement. This addendum builds on the previous work by analyzing two different cement "recipes" provided by industry partners using the techniques described in Kutchko et al. (2013). In addition, a series of checks were performed to ensure that a digital volume of sufficiently large dimensions was used for analysis in the foamed cement. Further research will correlate laboratory- and field-generated foamed cements and will attempt to develop a predictive relationship between gas distribution and physical properties.

1. INTRODUCTION

As discussed in Kutchko et al. (2013), foamed cement is a gas-liquid dispersion used in formations that are unable to support the annular hydrostatic pressure of conventional cement slurries. When these cements are used in the field, various additives are added to the cement slurry to enhance the stability of the gas bubbles within the cement/nitrogen mixture (Benge et al., 1996). The addition of foaming agents and foam stabilizers to foamed cement has been shown to improve the distribution of bubbles within the cured foamed cement (Benge et al., 1996).

This study builds upon previous work (Kutchko et al. 2013) to evaluate differences in the bubble size distribution (BSD) of two different recipes of foam cement commonly used in the field. The atmospheric-generated foamed cement evaluated by Kutchko et al. (2103) (foamed cement Recipe 1) is referred to as FCR1 in this addendum. The foamed cement Recipe 2, referred to as FCR2, was generated using a different amount and type of foaming agent. Both of these recipes were provided by industry partners for this study.

In addition to characterizing different atmospheric-generated foamed cement recipes, this study evaluates the effect of the volume analyzed in the BSD determination. A minimum volume of cement must be analyzed to accurately capture enough of the air voids to describe the BSD. This representative elemental volume (REV) analysis will provide future researchers with information that will allow for rapid, yet accurate, calculations to be performed.

2. METHODS

2.1 CEMENT SLURRY PREPARATION

Both foamed cement samples were prepared using a base slurry of Class H Portland cement (Lafarge, Joppa, IL) with a slurry density of 16.5 lb/gal (1.97 g/cm^3). These foamed cement recipes are commonly used in the Gulf of Mexico offshore wells. Foamed cement samples were prepared according to American Petroleum Institute (API) recommended practices 104-B as described in Kutchko et al. (2013). Four foam qualities, 10%, 20%, 30%, and 40% entrained air fractions, were mixed using two different industry-standard foaming agents. The eight different cements were mixed, cured, and cored using the methods described by Kutchko et al. (2013).

2.2 CEMENT CORE PREPARATION

One-inch diameter cores of the 10%, 20%, 30%, and 40% foam qualities were drilled to allow for scanning both cement recipes. These cores were subsequently subcored with a 6-mm diameter to allow for higher resolution scans. In total 16 scans were performed: 8 low-resolution (macro) scans of larger cores, and 8 high-resolution (micro) scans of the cores. Radial and axial photographs of the FCR1 cores (Figures 1–4) are shown in Kutchko et al. (2013). Each photograph includes a millimeter ruler for scale indication. Images of FCR2 samples are shown in Figures 1–4. Visually, both cement mixtures appeared similar with the exception that the hardened cement of the FCR2 cores was slightly lighter in color than the FCR1 samples. The increase in the individual void sizes from a 10% foam quality to a 40% is obvious without additional magnification in these figures as was the case for FCR1 cores in Kutchko et al. (2013).

Figure 1: Photographs of 25.4- and 6-mm diameter cores of 10% foam-quality FCR2 foamed cement Recipe 2 cores.

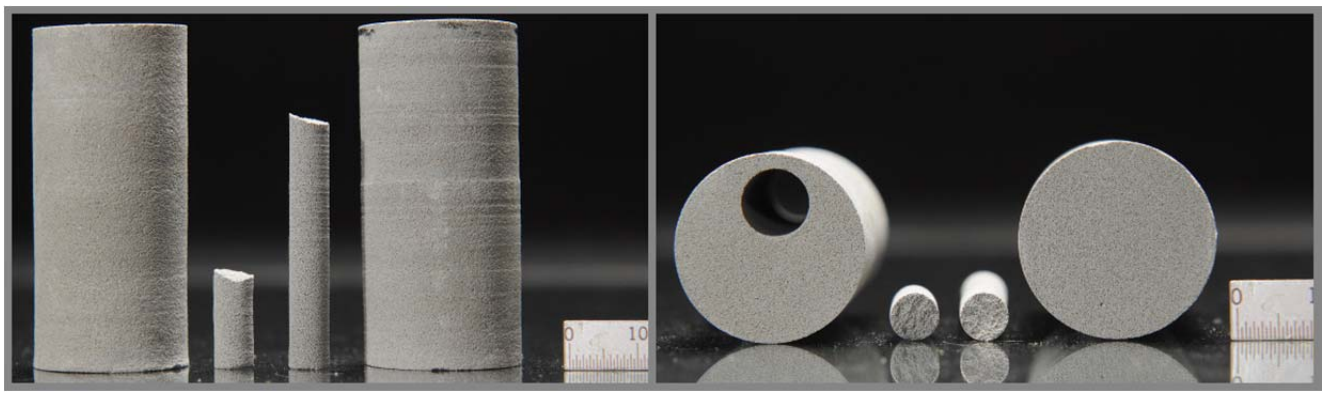

Figure 2: Photographs of 25.4- and 6-mm diameter cores of 20% foam-quality FCR2 foamed cement Recipe 2 cores.

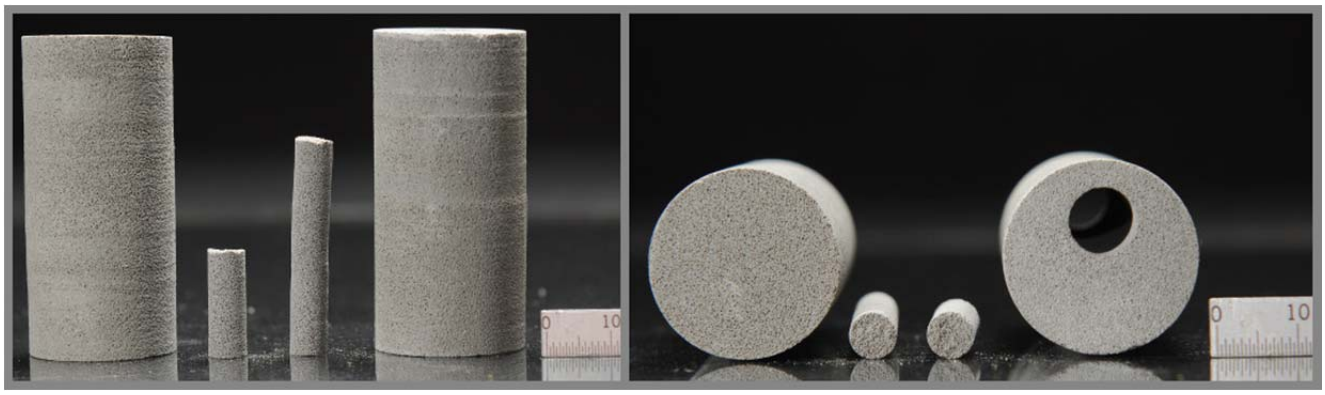

Figure 3: Photographs of 25.4- and 6-mm diameter cores of 30% foam-quality FCR2 foamed cement Recipe 2 cores.

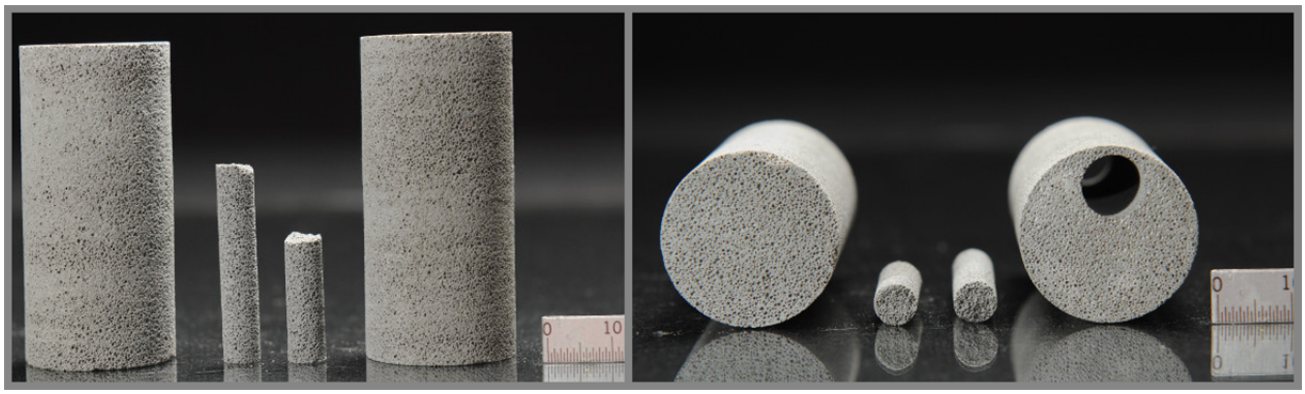

Figure 4: Photographs of 25.4- and 6-mm diameter cores of 40% foam-quality FCR2 foamed cement Recipe 2 cores.

2.3 CT SCANNING

All of the cores were scanned using a North Star Imaging M-5000 industrial CT scanner with the properties listed in Kutchko et al. (2013). Similar to the scans of the FCR1 cores, the reconstructed images of the 25.4-mm diameter FCR2 cores have a voxel resolution of 13.9 µm and the smaller subcores with a 6-mm diameter have a voxel resolution of 3.9 µm. The 10% foam quality FCR2 core sample scans had a slightly different voxel resolution of 14.3 µm for the 25.4- mm diameter cores and 4.3 µm for the 6-mm diameter cores. The CT scan reconstruction techniques and importation of slices into ImageJ (Rasband, 2012) for analysis were the same as was described by Kutchko et al. (2013).

2.4 DIGITAL IMAGING AND STATISTICAL ANALYSIS

The CT scans of the FCR2 cores shared many of the same characteristics as the FSC1 core scans discussed in Kutchko et al. (2013). The similarities include a variation in the grayscale values due to dense particles in the cement matrix, the cement matrix itself, and pore fluids. These variations in the FCR2 grayscale values are shown pictorially in Figure 5 and Figure 6 with 2-D slices of the reconstructed CT scans. The detailed threshold technique described by Kutchko et al. (2013) was employed on these different foamed cement cores to test the rigor of the technique and to ensure that this analysis could be used on various samples with the same level of confidence.

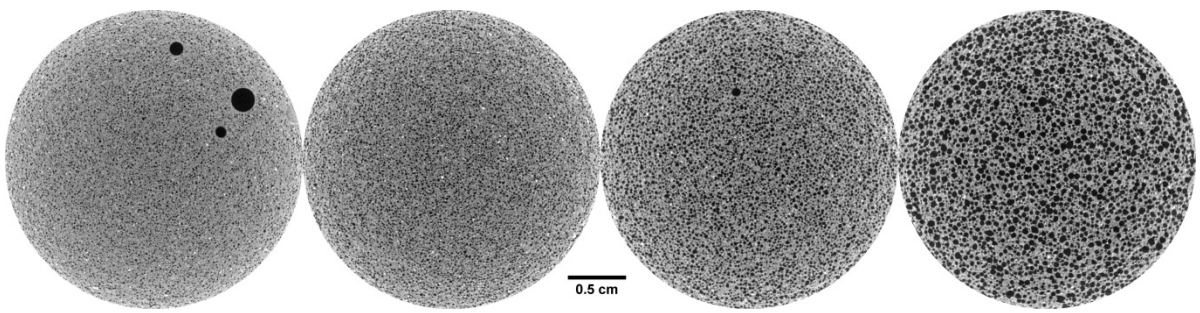

Figure 5: 2-D slices of reconstructed 13.9-µm resolution CT scans of the 25.4-mm diameter samples of 10%, 20%, 30%, and 40% foam-quality FCR2 foamed cement Recipe 2 cores (left to right).

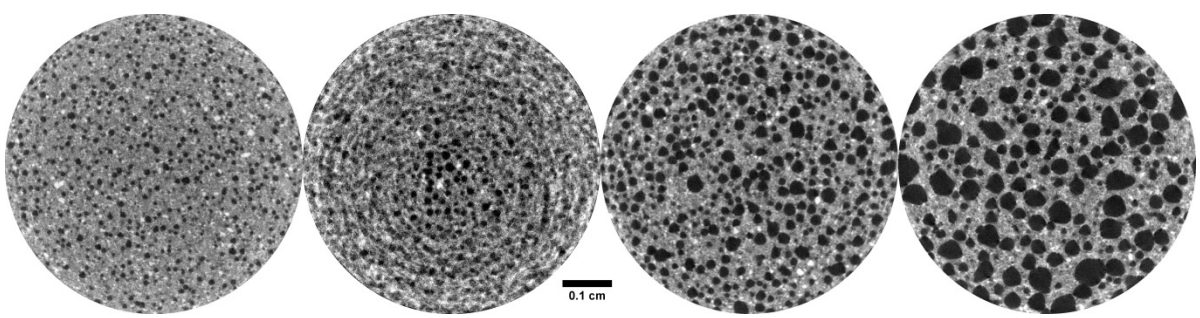

Figure 6: 2-D slices of reconstructed 3.9-µm resolution CT scans of the 6-mm diameter samples of 10%, 20%, 30%, and 40% foam- quality FCR2 foamed cement Recipe 2 cores (left to right).

In the BSD and structure analysis described by Kutchko et al. (2013), due to the large amount of processing power required for the analyses, a small subsection of each scan was chosen (Table 1). Different regions of interest (ROI) and thus volumes of analysis were chosen from FCR2 cores, primarily due to the ability to evaluate a larger ROI with increased processing power. The larger ROIs used for the FCR2 analyses resulted in a total volume studied of 0.030 $cm^3$and 0.580 cm^3 for the micro- and macroscans, respectively while the previous analysis of the FCR1 cores resulted in total volumes of 0.013 cm^3 and 0.781 cm^3 for the micro- and macroscans. The different volume of analyzed cement was used to show that all calculations were performed on volumes greater than the REV of the foamed cement. A REV is the smallest subvolume of a porous medium that contains the same characteristics (i.e., porosity, BSD, etc.) as the entire volume.

Edge-adjacent bubbles were eliminated from the analysis of the 10% foam quality samples to decrease the impact of partial bubble volumes. The increasingly interconnected nature of bubbles in the 20%, 30%, and 40% foam prevented such selection of data and edge-adjacent bubbles had to be retained for analysis.

The effect of bin-size selection on bubble distributions was shown in Kutchko et al. (2013). In the analysis of the FCR2 cores and compared to the previously analyzed atmospherically generated foamed cement cores, a bin size of 50,000 voxels was consistently used. As in Kutchko et al. (2013), bubbles less than 10 voxels in size were negligible in their contribution to the overall porosity and showed no appreciable influence on BSD; therefore, bubbles less than 10 voxels were not included in the analysis.

Table 1: Scan resolutions and resultant analysis volumes for FCR1 and FCR2 foamed cement recipe cores

Foam Quality (%)	Cement Recipe	Source	Resolution (µm)	Volume (cm^3)
10	1	Micro	3.7	0.013
10	**1**	**Macro**	**13.5**	**0.781**
10	2	Micro	3.9	0.030
10	**2**	**Macro**	**14.5**	**0.580**
20	1	Micro	3.7	0.013
20	**1**	**Macro**	**13.5**	**0.781**
20	2	Micro	3.9	0.030
20	**2**	**Macro**	**13.5**	**0.580**
30	1	Micro	3.7	0.013
30	**1**	**Macro**	**13.5**	**0.781**
30	2	Micro	3.9	0.030
30	**2**	**Macro**	**13.5**	**0.580**
40	1	Micro	3.7	0.013
40	**1**	**Macro**	**13.5**	**0.781**
40	2	Micro	3.9	0.030
40	**2**	**Macro**	**13.5**	**0.580**

3. RESULTS

To test the accuracy of CT-derived image data, the experimentally determined porosity of the cement was compared with porosity data derived from CT images (Figure 7). The correlation was of remarkably good quality between the experimental gas fraction and the measured CT air volume. For 10 and 20% foam-quality cements, the calculated porosity values were within 1.3% of experimental gas volume percentages for all samples with the exception of FCR2 10% micro which was 3.6% above expected and FCR2 20% macro which was 2.3% below expected. The 30% foam-quality cement varied the most between the two recipes with scans of FCR1 cores having higher than expected porosity. The FCR1 cores were calculated at over 33% with both the macro- and microscales, while FCR2 cores were calculated to within 1.5% of the expected 30% foam-quality cement at both scales. For the 40% foam-quality cements, both recipes had calculated porosities higher than expected, with the FCR1 macro-resolution having a maximum of 46.22%.

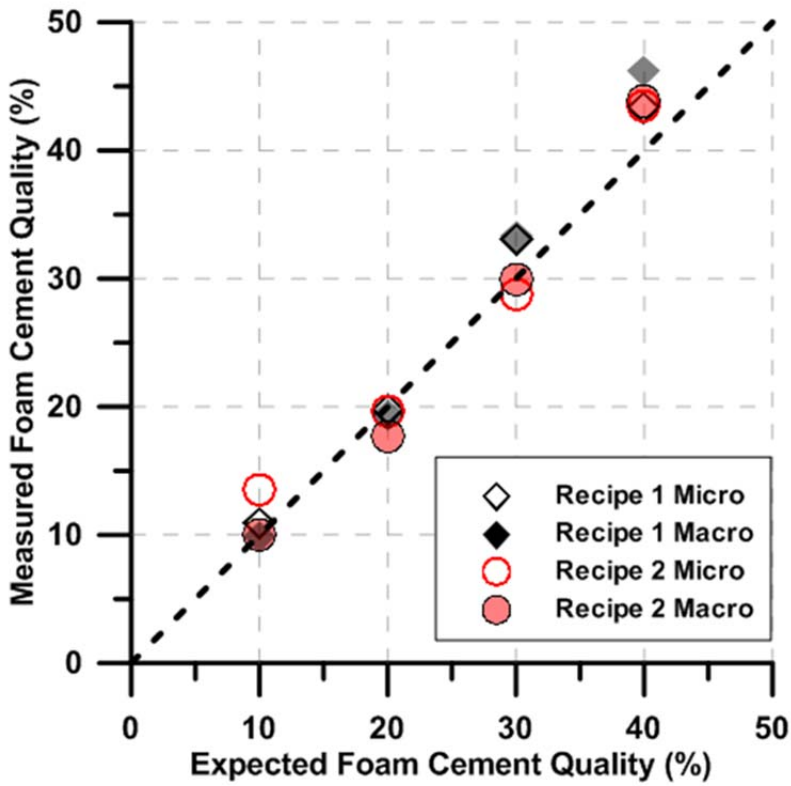

Figure 7: CT-derived porosity vs. entrained air fraction with the dashed line denoting a linear relationship with slope = 1. The data are from low-resolution (macro) and high-resolution (micro) scans of both foamed cement recipes.

The BSD of both foamed cement recipes are shown in Figures 8 and 9. The 30% foam-quality cement for both FCR1 and FCR2 cement recipes is anomalous due to the nearly identical slopes and relative overlap of the micro- and macroscans of the BSDs. These distributions are shown separately in Figure 8. Additionally, the inflection points of the 30% foam-quality BSD observed at both scales overlap, which implies that both the small and larger volumes of the cement are greater than the REV of the samples. If the volume analyzed was smaller than an REV, a difference in the BSD distribution would be expected between the measurements.

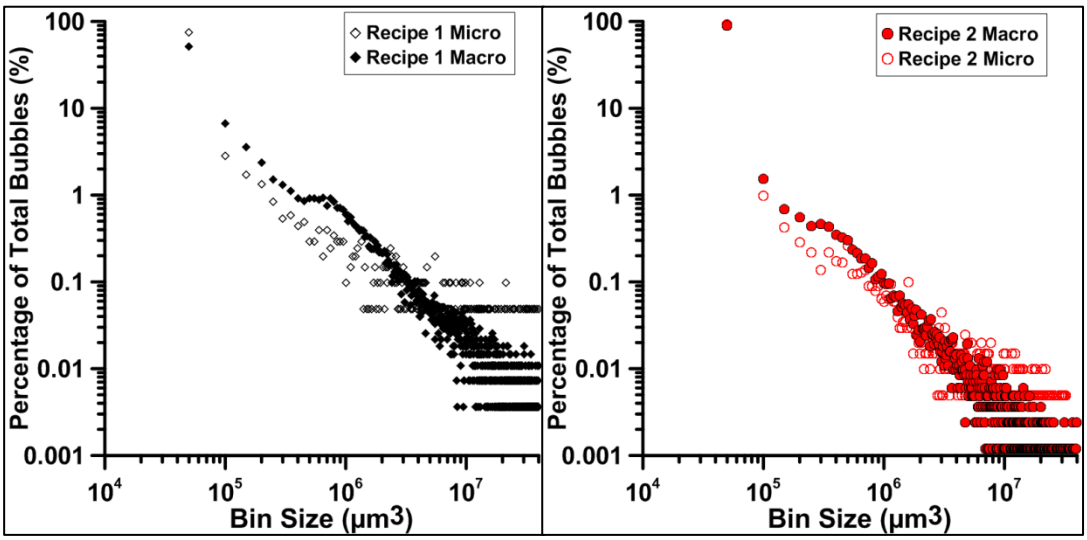

Figure 8: Log-log BSD plots of the 30% foam-quality samples. For the FCR1 and FCR2 foamed cement recipes, the micro- and macro-BSD are extremely similar.

Comparisons of the 10%, 20%, and 40% foam-quality BSDs for both the microscans and the macroscans are shown in Figure 9. The bubble distributions are similar in all cases with the smallest measured individual bubble volumes accounting for over 95% of the total measured bubbles. In all cases, the microscans captured a larger number of small bubbles, and the remaining BSD occupied a smaller percentage of the total bubbles. This result led to a consistently lower slope of the BSD for the microscans, with the occurrence of large bubbles accounting for a smaller percentage of the BSD. High-quality cements have larger percentages of larger bubble sizes in the BSD due to those samples having more interconnected bubble volumes; the larger volumes may be inflated because of the thin menisci that separate bubbles, which lead to aggregation during image processing due to it being nearly impossible to isolate those zones. A comparison the BSD of the FCR1 cement recipe to the BSD of FCR2 cement recipe shows that the BSDs are very similar for all foam qualities evaluated.

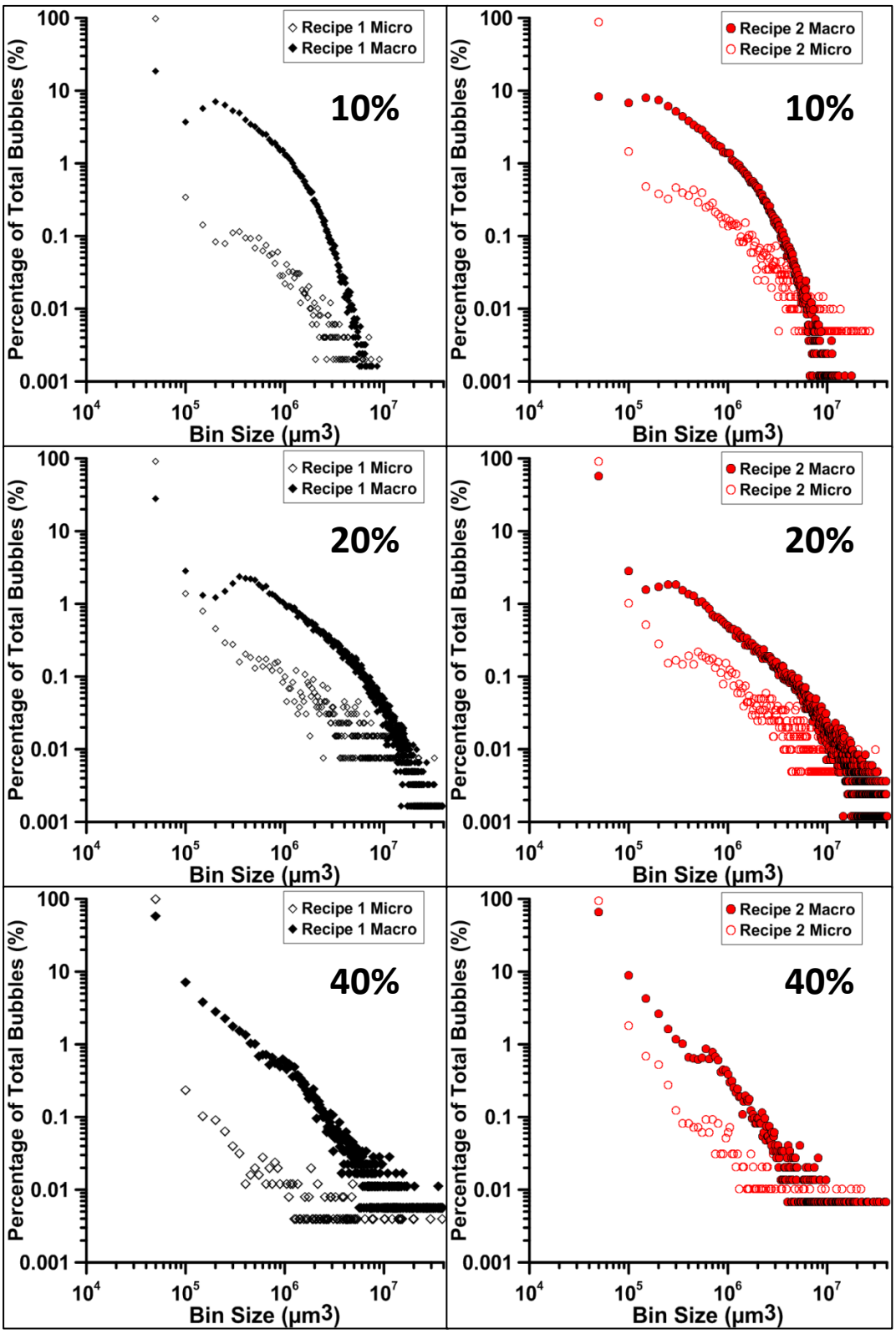

Figure 9: Log-log BSD plots of the 10%, 20%, and 40% foam-quality samples. For the FCR1 and FCR2 foamed cement recipes, the micro- and macro-BSD have similar distributions. In all cases, the microscans captured a larger number of small bubbles, and the remaining BSD occupied a smaller percentage of the total bubbles.

Figure 10 shows a comparison of the microscan vs. macroscan for both recipes. As was shown in Figure 9, the smallest measured bubbles comprise the largest percentage of the bubbles, and this affects the BSD of the remaining voids. The BSDs of the different recipes are remarkably similar for all the qualities evaluated. This result indicates that the changes in BSD due to the type of foaming agents and additives used in these two recipes do not dramatically change the bubble structure of atmospherically generated foamed cement.

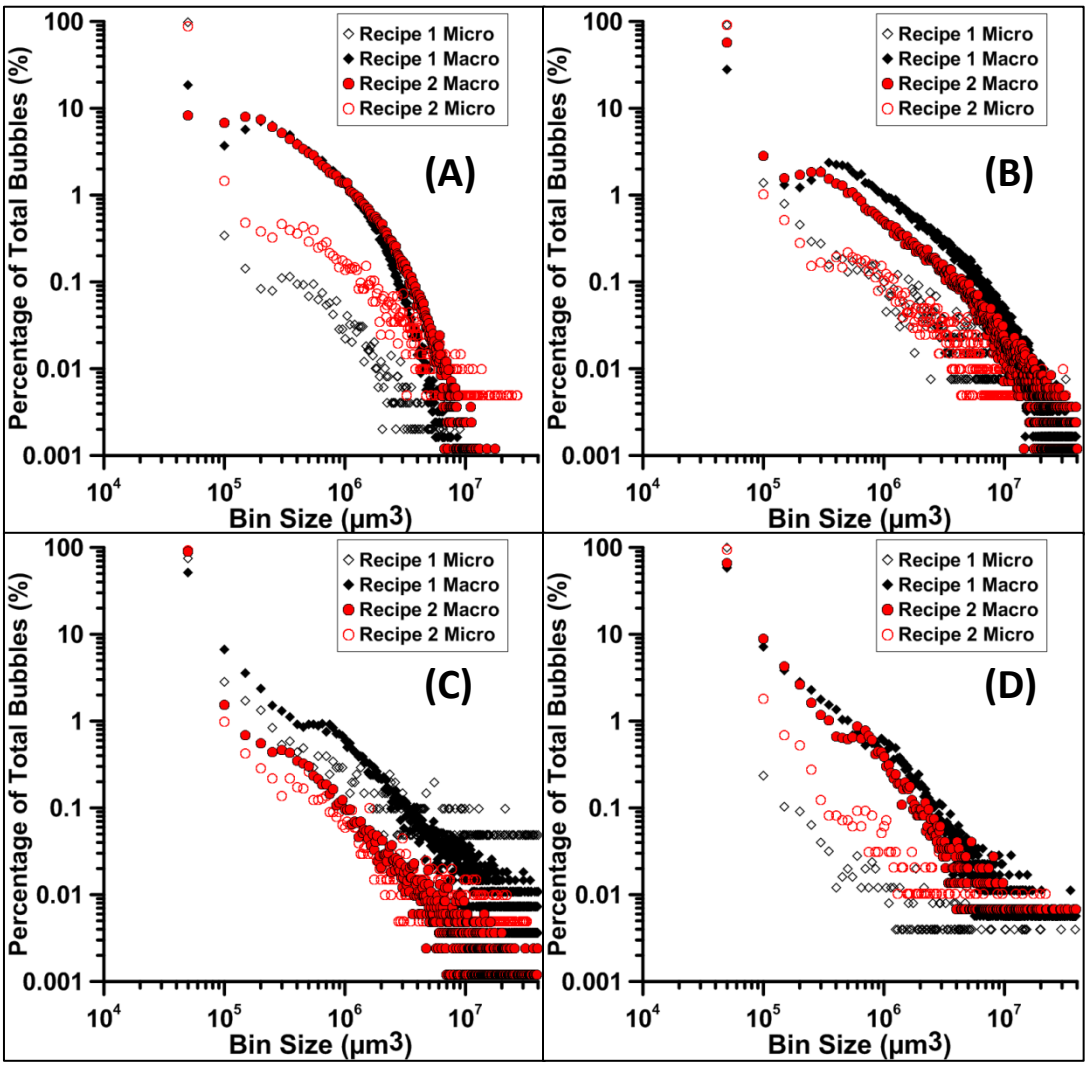

Figure 10: Log-log BSD plots for the FCR1 and FCR2 foamed cement recipes with the BSDs overlaid. Scan resolutions for the FCR1 and FCR2 foamed cement recipe cores are 13.5 µm for the macroscans. The FCR1 microscans have a resolution of 3.7 µm and the FCR2 microscan resolutions are 3.9 µm. A) 10% foam quality, B) 20% foam quality, C) 30% foam quality, and D) 40% foam quality.

4. DISCUSSION

As discussed by Kutchko et al. (2013), the atmospherically generated foam cements' experimentally determined entrained air, via CT imaging and analysis, closely approximates the expected foam qualities. The analysis of the FCR2 cement recipe, performed using the same methodology as in the initial report, supports the original findings that the proposed technique for digital porosity evaluation is accurate. As in the primary study, the higher quality cements for the FCR2 cement recipe had more interconnected bubble volumes; thus, BSDs skewed towards the larger bubbles.

The results also show that for the two atmospheric-generated cement recipes studied, the BSD does not vary greatly; gas content and generation techniques appear to control the shape of the final BSD. However, this is not a complete evaluation of interconnectivity and does not suggest that the cements are similar in their respective permeabilities and interconnectivity.

Using two different ROIs for the analysis of FCR1 and FCR2 cement recipes, while retaining nearly identical BSDs for each quality, indicate that the REVs of the studied cements are below the minimum volume used for analysis (0.013 cm^3 for microscans and 0.58 cm^3 for macroscans). Of course, this REV will be dependent on the voxel size of the reconstructed CT image; smaller voxel sizes enable more small bubbles to be isolated and require a smaller overall volume to be analyzed due to processing capabilities.

This study confirms that high-resolution CT imaging and statistical analysis can be used to determine the quality and gas distribution of various foamed cements. In both foamed cement recipes tested, the CT-measured entrained air volume was consistent with the foam quality, which ensures that the CT-derived image data are accurate and provides a reliable methodology to study the mesostructure and stability of foamed cements. As mentioned by Kutchko et al. (2013), this methodology is currently being applied to field-generated foamed cements. Correlations between atmospheric- and field-generated foamed cements and their physical properties are needed to develop predictive in situ models of foamed cement stability under wellbore conditions. This research will provide researchers, regulators, and the industry with the knowledge to ensure the safe operation and integrity of wells in which foamed cement recipes are used.

5. REFERENCES

API. *API Recommended Practice 10B-4. Recommended Practice on Preparation and Testing of Foamed Cement Slurries at Atmospheric Pressure, First Edition*; American Petroleum Institute: Washington, DC, 2004.

Benge, O. G.; McDermott, J. R.; Langlinais, J. C.; Griffith, J. E. Foamed cement job successful in deep HTHP offshore well. *Oil and Gas Journal* **1996,** *94*, 58–63.

Kutchko, B.; Crandall, D.; Gill, M.; McIntyre, D.; Spaulding, R.; Strazisar, B.; Rosenbaum, E.; Haljasmaa, I.; Benge, G.; Cunningham, E.; DeBruijn, G.; Gardner, C. *Computed Tomography and Statistical Analysis of Bubble Size Distributions in Atmospheric-Generated Foamed Cement*; NETL-TRS-2-2013; EPAct Technical Report Series; U.S. Department of Energy, National Energy Technology Laboratory: Morgantown, WV, 2013; p 28.

Rasband, W. S. ImageJ. http://imagej.nih.gov/ij/ (accessed 2013), U.S. National Institutes of Health: Bethesda, MD, 1997–2012.

The National Energy Technology Laboratory (NETL) conducts cutting-edge energy research and technology development and analyzes energy systems and international energy issues for the U.S. Department of Energy. The NETL-Regional University Alliance (NETL-RUA) is an applied research collaboration that combines NETL's energy research expertise with the broad capabilities of five nationally recognized, regional universities: Carnegie Mellon University (CMU), The Pennsylvania State University (PSU), University of Pittsburgh (Pitt), Virginia Polytechnic Institute and State University (VT), and West Virginia University (WVU), and the engineering and construction expertise of an industry partner (URS). The NETL-RUA leverages its expertise with current fossil energy sources to discover and develop sustainable energy systems of the future, introduce new technology, and boost economic development and national security.

Brad Tomer
Acting Director
Strategic Center for Natural Gas and Oil
National Energy Technology Laboratory
U.S. Department of Energy

Maria Vargas
Deputy Director
Strategic Center for Natural Gas and Oil
National Energy Technology Laboratory
U.S. Department of Energy

Roy Long
Technology Manager
Strategic Center for Natural Gas and Oil
National Energy Technology Laboratory
U.S. Department of Energy

Elena Melchert
Program Manager
Oil and Gas Production
Office of Fossil Energy
U.S. Department of Energy

Cynthia Powell
Director
Office of Research and Development
National Energy Technology Laboratory
U.S. Department of Energy

Timothy McNulty
Associate Vice-President for
Government Relations
Carnegie Mellon University

Henry Foley
Vice President for Research
The Pennsylvania State University

George Klinzing
Vice Provost for Research
University of Pittsburgh

Robert Walters
Vice President for Research
Virginia Polytechnic Institute and State
University

Fred King
Vice President for Research and
Economic Development
West Virginia University

Kevin Donovan
RES Program Manager
URS Corporation